

Analyzing the shear strength parameters of the Chiu-fen-erh-shan landslide: integrating strong-motion and GPS data to determine the best-fit accelerogram

Jian-Hong Wu · Hung-Ming Lin

Received: 14 February 2008 / Accepted: 11 August 2008 / Published online: 3 September 2008
© Springer-Verlag 2008

Abstract This study adopts the Chiu-fen-erh-shan landslide as a case study for incorporating comprehensive accelerograph and global positioning system (GPS) data to determine the best-fit acceleration data for analyzing a rock avalanche. Previous investigations indicate that the distance from an accelerograph to a landslide site is crucial to determining the best-fit acceleration data to use in conducting a seismic analysis. Unfortunately, the Chiu-fen-erh-shan landslide and its nearest accelerograph station are located in different geological zones. Thus, GPS data were compared to the displacements derived from the accelerograms of nearby monitoring stations to help select the best accelerograph data. This emphasizes that a high density distribution of accelerographs and GPS installations are essential to acquire the best data for the seismic analysis, especially in complex geological zones. After applying the best-fit accelerogram to Newmark's sliding model and an empirical displacement attenuation formula to back-calculate the shear strength parameters of the sliding surface, a cohesion of 0 kPa and friction angle of the sliding surface of 24.8° were found for this landslide.

Keywords Chiu-fen-erh-shan landslide · Chi-Chi earthquake · Accelerograph · GPS · Displacement · Newmark

Introduction

The calamitous Chi-Chi earthquake (1999) and Chuetsu earthquake (2004) triggered massive landslides, such as the Chiu-fen-erh-shan landslide (Wang et al. 2003; Wu 2007), the Tsao-ling landslide (Chigira et al. 2003), and the Shiotani landslide (Chigira and Yagi 2006). Because seismic acceleration time histories are frequently recorded to identify the characteristics of an earthquake, these data have become crucial for analyzing seismically induced landslides. However, it should come as no surprise that predicting the best location to record seismic behavior of future earthquake-induced landslides remains difficult. Crespellani et al. (2003) mentioned that the most reliable accelerograms for geotechnical applications are obtained from strong ground motion recorded by accelerograph stations located near the site of the event.

To analyze seismically induced landslides, Cai and Bathurst (1996) concluded that force-based pseudo-static and displacement-based sliding block methods are available techniques for assessing ground performance under seismic loading. The simplest approach for dynamic analysis of slopes is the force-based pseudo-static analysis. In the pseudo-static approach, the safety factor against sliding is obtained by including horizontal and vertical forces in the static analysis. These forces are usually expressed as a product of the horizontal or vertical Peak Ground Accelerations (PGA) and the weight of the potential sliding mass.

Turning to the Chiu-fen-erh-shan landslide, Fig. 1 illustrates the spatial distribution of free-field accelerograph

J.-H. Wu (✉)
Department of Civil Engineering,
National Cheng Kung University,
No. 1, University Road, Tainan, Taiwan
e-mail: jianhong_wu@yahoo.com; jhwu@mail.ncku.edu.tw

J.-H. Wu
Sustainable Environment Research Center,
National Cheng Kung University, Tainan, Taiwan

H.-M. Lin
Department of Construction and Facility Management,
Leader University, Tainan, Taiwan

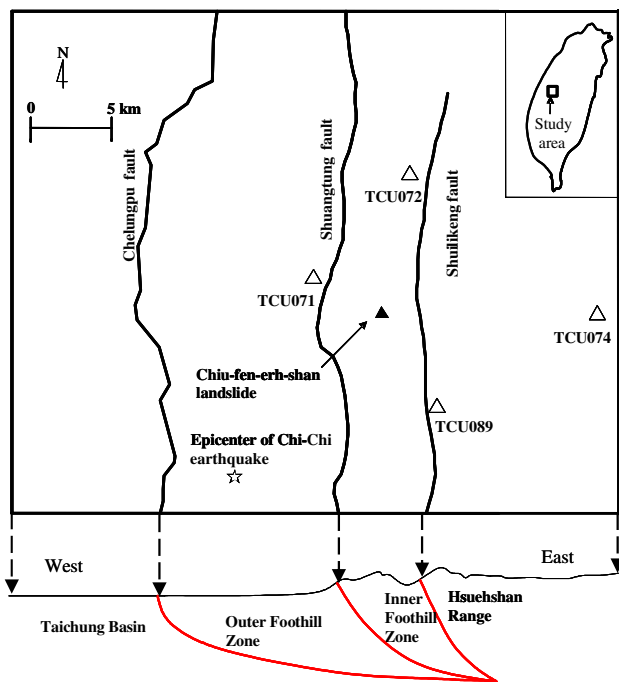


Fig. 1 The spatial and geological distribution near the Chiu-fen-erh-shan landslide

stations, TCU071, TCU072, TCU074, and TCU089 near the site of the landslide. Hung et al. (2000) applied the PGA from TCU072, in both the vertical and horizontal directions, to a force-based pseudo-static analysis. Back-calculating the shear strength parameters of the sliding surface, they found the cohesion, c , at the surface to be 235 kPa and the angle of the surface, ϕ , to be 28° . Additionally, Shou et al. (2001) interpolated the vertical and horizontal accelerations of TCU071 and TCU089, and applied the shear strength parameters obtained from laboratory tests to investigate the stability of Chiu-fen-erh-shan landslide slope before and during the Chi-Chi earthquake. That analysis showed that the safety factor of the slope was 1.77 before the earthquake but fell to 0.5 during the Chi-Chi earthquake. Later, Chang et al. (2005) selected the PGA of TCU071, TCU089 and TCU072 (enclosing the landslide area) for inclusion in block-on-slope thermo-mechanical analysis. The original uncorrected strong-motion records were filtered by baseline corrections and band-pass filtering using Butterworth filter cut-off frequencies [>0.2 and <20 Hz] before further analysis. Their study revealed that the initiation and propagation of earthquake-induced landslides are mainly controlled by the peak and residual shear strength parameters of the sliding surface.

The displacement-based sliding block method (Newmark 1965) is an alternative method that ascertains the stability of slopes during an earthquake based on estimating the extent of displacement of a sliding block moving along a failure surface. Different from merely considering the PGA in the force-based analysis, the seismic acceleration time history is

a crucial datum for evaluating the movement of a slope during an earthquake in this displacement-based method because the sliding block moves when the triggering forces generated by gravity and seismic accelerations exceed the shear resistance of the sliding surface. Consequently, not only distance and local conditions, but also source mechanisms and wave propagation, as well as local conditions significantly affect all seismic parameters (frequency content, duration, peak ground acceleration). Huang et al. (2001) investigated the effect of surface-normal acceleration on the initiation of the Chiu-fen-erh-shan landslide using the seismic data from station TCU089. Their study showed that the surface-normal acceleration, currently not considered by dynamic slope-stability analysis methods, significantly influences the initiation of a landslide. Ma et al. (2003) mentioned that the stations near the largest observed surface offset of Chelungpu fault recorded large ground velocities and displacements (up to 4.5 m/s and 12 m, respectively); the largest such values ever instrumentally measured. In addition, Boore (2001) and Chen and Loh (2007) identified that after the removal of the pre-event mean in the near-field acceleration of Chi-Chi earthquake, a linear velocity trend still remained—which indicated the latter half of the acceleration has a different baseline than the pre-event portion. The source mechanism of the shifts in zero level is unknown but, in at least one case, it is almost certainly due to tilting of the ground caused by the violent ground vibrations in the near-field area (Boore 2001; Graizer 2005). Finally, note that the cohesion and friction angle parameters presented in the available literature and summarized in Table 1. These vary significantly: 0–235 kPa for the cohesion, 21° – 30.8° for the friction angle. The heterogeneity of rock samples and different designs for laboratory tests are most likely the main reasons for these variations but one should bare in mind that two of the studies, Hung et al. (2000) and Wu et al. (2005), back-calculated the shear strength parameters of the Chiu-fen-erh-shan landslide slope using the force-based pseudo-static method.

Obviously, this is a complex event in a complex region for which no consensus about the fundamental descriptive parameters of the landslide has emerged. This paper attempts clarify our understanding of the Chiu-fen-erh-shan landslide. We will use the Newmark sliding model to back-calculate the shear strength parameters of Chiu-fen-erh-shan landslide slope, but first we will review the distribution of nearby accelerographs and their geological conditions to identify other selection criteria, besides distance, which can be used to determine the optimal accelerographs for input to the model. In addition, the co-seismic permanent ground displacements will be determined by double integration of the baseline corrected seismic accelerations of each nearby accelerograph and compared with the data of adjoining GPS stations. These

Table 1 A summary of shear strength parameters for the Chiu-fen-erh-shan landslide

References	Shear strength parameters	Remark
Chen (2000)	$c = 20$ kPa; $\phi = 22\text{--}28^\circ$	–
Hung et al. (2000)	$c = 235$ kPa; $\phi = 28^\circ$	Pseudo-static analysis
Shou et al. (2001)	Residual shear strength, $c_r = 50$ kPa, $\phi_r = 30.8^\circ$	Direct shear test
Shou and Wang (2003)	Residual shear strength, $c_r \approx 0$ kPa, $\phi_r = 30.8^\circ$	Direct shear test
	Residual shear strength (one-month saturated)	Direct shear test
	$c_r \approx 0$ kPa, $\phi_r = 27.3^\circ$	
Wu et al. (2005)	$c = 20$ kPa; $\phi = 21^\circ$	Pseudo-static analysis

too will be input to Newmark sliding model and the empirical displacement attenuation formula to assess the earthquake-induced displacements and the shear strength parameters of the sliding surface of Chiu-fen-erh-shan landslide.

Geological outline of Chiu-fen-erh-shan landslide slope

Taiwan is located at the edge of Eurasia and Philippine plates. Tectonic forces have resulted in a complex geology with several geological zones separated by fault lines. The Chiu-fen-erh-shan landslide slope is located in central Taiwan, part of the hanging wall of the Chelungpu fault between the Shuilikeng and Shuangtung faults (Fig. 1). Huang et al. (2000b) believed that the Shuilikeng and Shuangtung faults divided western central Taiwan into three geological zones from east to west: the Hsuehshan range, inner and outer foothill zones. The Hsuehshan range is composed of Paleogene sub-metamorphic rocks. The inner foothill zone mainly consists of Miocene sandstone and shale with limited Pliocene sandstone. The outer foothill zone is primary composed of Pliocene and Pleistocene sandstone, shale and conglomerate rocks.

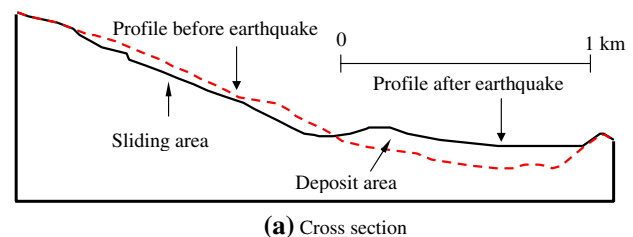
The study area is roughly 12 km north-northeast from the epicenter of the Chi-Chi earthquake, as shown in Fig. 1. In addition, Fig. 2a presents a cross section of Chiu-fen-erh-shan landslide slope obtained from topographic contours. This view is comprised of sliding and deposit areas before and after the dip-slope rock avalanche triggered by the Chi-Chi earthquake ($M_L = 7.3$). Figure 2b shows a side view of the slope in 2005. Fractured, weathered rocks and soil slid along a bedding interface when the slope failed on 21 September 1999. The slope failure engulfed 195 ha and buried 39 residents.

The Changhukeng shale is the parent rock on the slope (Shou et al. 2001). The local strata consist of alternating sandstone and shale layers. The slip surface of the Chiu-fen-erh-shan landslide strikes parallel to the bedding plane whose dip angles are $20\text{--}36^\circ$ (Chen 2000; Huang et al. 2000a; Shou et al. 2001; Wang et al. 2003). Furthermore, investigations by Wang et al. (2003) identified abnormal

cracks on the Chiu-fen-erh-shan landslide slope from the topographic map before the Chi-Chi earthquake. The spatial distribution of the cracks correlated well with the boundaries of the landslide. Therefore, the slope can be assumed to have been unstable before the earthquake and the shear strength of the sliding surface to be in its residual state.

Nearby accelerograph and GPS stations

At the time of Chi-Chi earthquake, Taiwan's digital accelerograph network, monitored by the Central Weather Bureau of Taiwan, collected seismic accelerations and 453 free-field acceleration records have been released (<http://www.cwb.gov.tw/>). Simultaneously, the co-seismic



(a) Cross section
(b) Side view taken in 2005
Fig. 2 The Chiu-fen-erh-shan landslide slope

displacements of 285 geodetic control stations in Taiwan, under the auspices of Taiwan Bureau of Land Survey, were determined by GPS (Yang et al. 2000). The extensive set of seismic accelerations and displacements provide valuable records for the seismic analysis.

The spatial distribution of accelerograph and GPS stations

Figure 3 illustrates the spatial distribution of available free-field accelerographs installed in Taiwan (Shin et al. 2000). Boore (2001) mentioned that this strong-motion network acquired an exhaustive set of ground motion data during the Chi-Chi earthquake. Thus, the database provides valuable information for determining the best-fit strong-motion data for seismically induced landslide analysis. The free-field digital accelerograph stations TCU071, TCU072, TCU074 and TCU089 are near the Chiu-fen-erh-shan landslide site (Fig. 1). Table 2 lists the distance from the landslide to each station. The pre-event offset corrected three-component accelerations from specific accelerograph stations are showed in Figs. 4, 5, 6 through 7. No remarkable features are evident to identify the best-fit data directly from accelerations.

Many studies have examined the slope stability of the Chiu-fen-erh-shan landslide using strong-motion data from different stations. Hung et al. (2000) used the TCU072 data, while Shou et al. (2001) interpolated the TCU071 and TCU089 data. Kondo and Hayashi (2002) and Huang et al. (2001) utilized the TCU089 data. Chang et al. (2005) integrated accelerations from TCU071, TCU072, and TCU089. However, the seismic characteristics of the different stations have not been investigated, although source mechanisms, wave propagation, and local conditions significantly affect all seismic parameters (Crespellani et al. 2003).

Unfortunately, the availability of an additional index to present the source mechanisms, wave propagation, and local conditions in judging the most reliable accelerograph remains an unaddressed problem for geotechnical engineers. Fortunately, besides the free-field digital accelerograph stations, earthquake scientists also have the GPS to monitor regional tectonic movement in Taiwan (Fig. 8). Yang et al. (2000) accurately determined the co-seismic displacements of earth surface during the Chi-Chi earthquake with geodetic data recorded by the dense Taiwanese GPS network before and after the earthquake. The pre-earthquake data were obtained between 1995 and 1998 from global and regional permanent GPS tracking networks, as well as at Taiwan's first- and second-order geodetic control stations. While, the post-earthquake data including field surveys at geodetic control points in central Taiwan and continuous observations at the

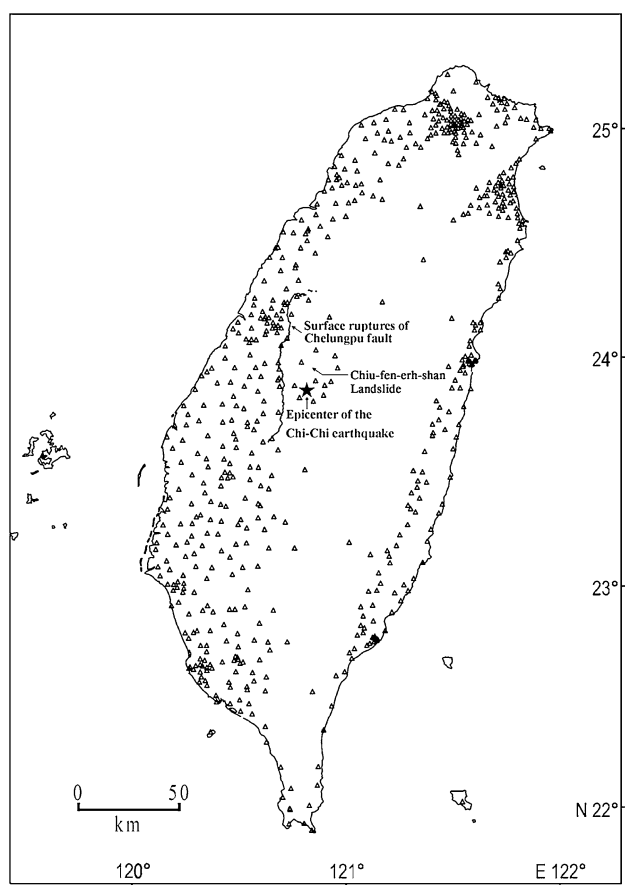


Fig. 3 Locations of the free-field digital accelerograph stations

Table 2 Distances of adjoining acceleration stations from the Chiu-fen-erh-shan slope

Acceleration station	Distance from Chiu-fen-erh-shan slope (km)
TCU071	5.3
TCU072	9.0
TCU074	12.5
TCU089	5.9

regional GPS tracking network stations gathered within one month of the earthquake. The abundant information contained in the available GPS data could be further inverted to determine the rupture geometry and slip distribution associated with the Chi-Chi earthquake. As a result, these can act as an index in judging the most reliable accelerograph for Chiu-fen-erh-shan landslide analysis.

Figure 9 and Table 3 display co-seismic ground displacements in the study area as measured by the GPS stations. In Fig. 9a, horizontal displacements show that all GPS stations moved northwestward coincidentally. However, the directions of vertical displacements were

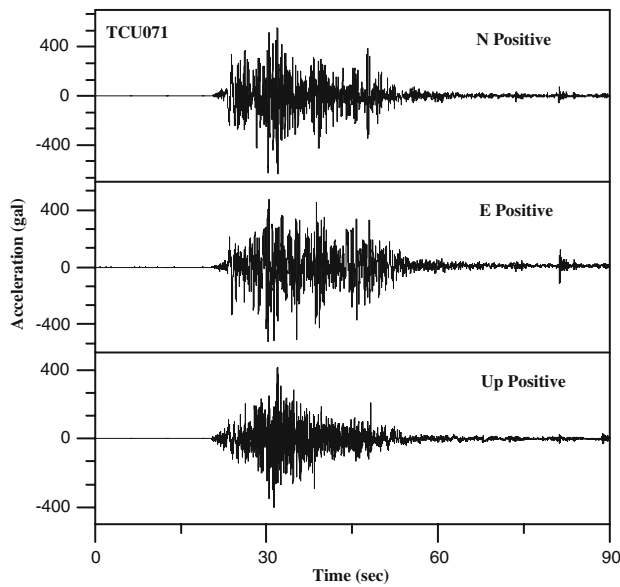


Fig. 4 Three components of seismic accelerations at TCU071

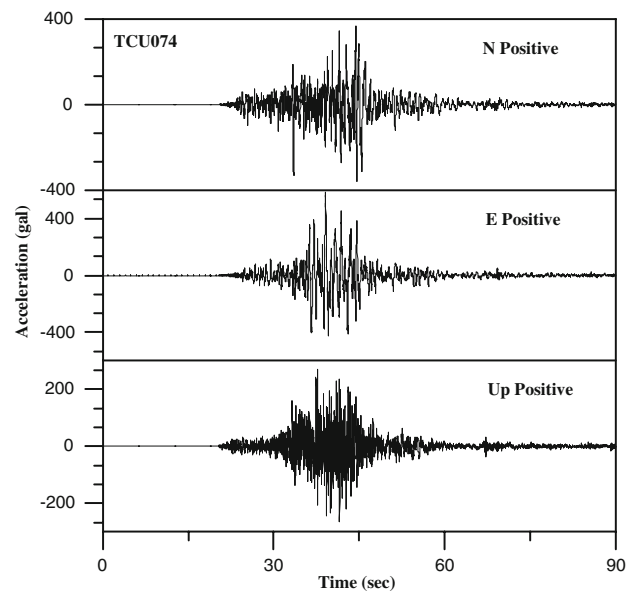


Fig. 6 Three components of seismic accelerations at TCU074

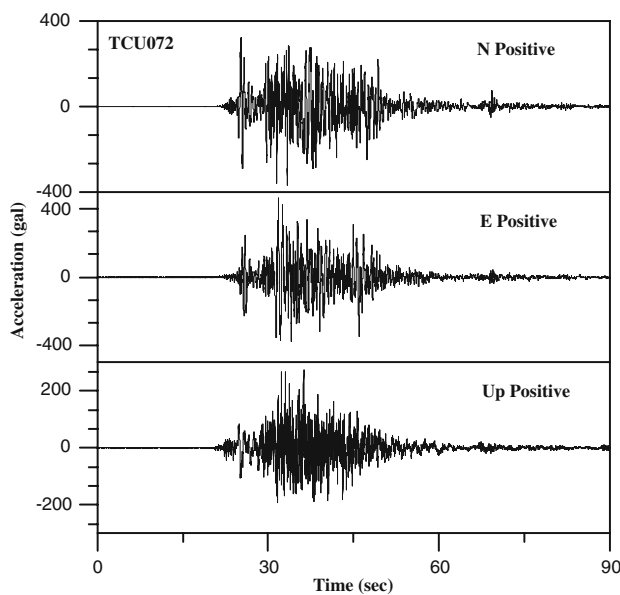


Fig. 5 Three components of seismic accelerations at TCU072

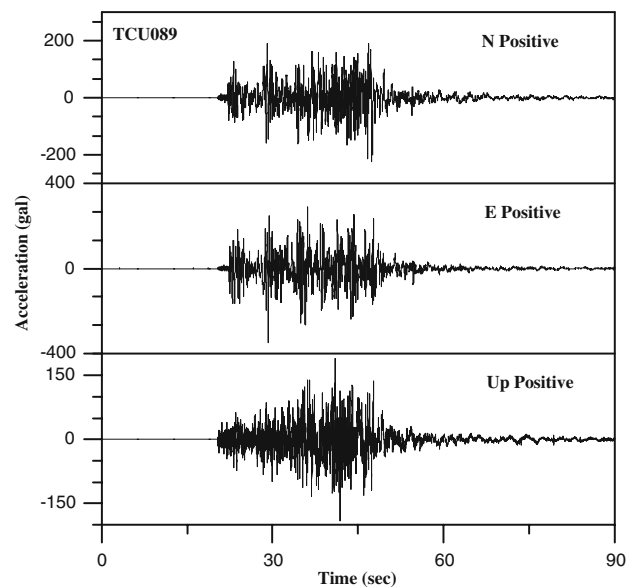


Fig. 7 Three components of seismic accelerations at TCU089

inconsistent (Fig. 9b). Three vertical displacement zones, separated by the Shuangtung and Shuilikeng faults, as described above, can be seen in the GPS results. Large upward displacements occurred in the outer foothill zone west of Shuangtung fault, while small downward displacements were distributed in the Hsuehshan range east of the Shuilikeng fault. Stations M501, M303, and M426 form a boundary between the regions of upward and downward motions. Thus, the GPS data for vertical displacement measurements are a useful tool in this study for determining the best-fit acceleration data.

Co-seismic permanent ground displacements

The displacements of the ground surface can be obtained by double integrating seismic accelerations. However, Boore (2001) showed that velocity and displacement derived from the near-field seismic accelerations of the Chi-Chi earthquake drifted (Fig. 10) when only a simple pre-event offset correction is applied. One assumes a change to zero acceleration likely caused these drifts. The mechanism causing the zero level shift remains unknown, although the tilting ground during this strong earthquake is

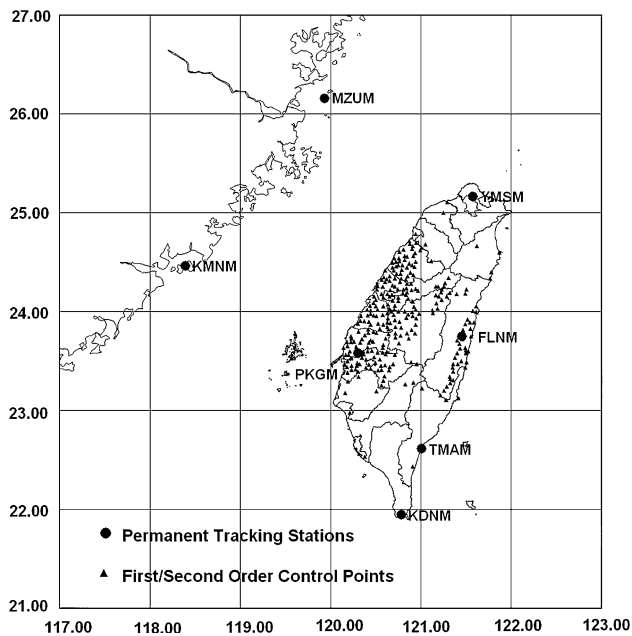
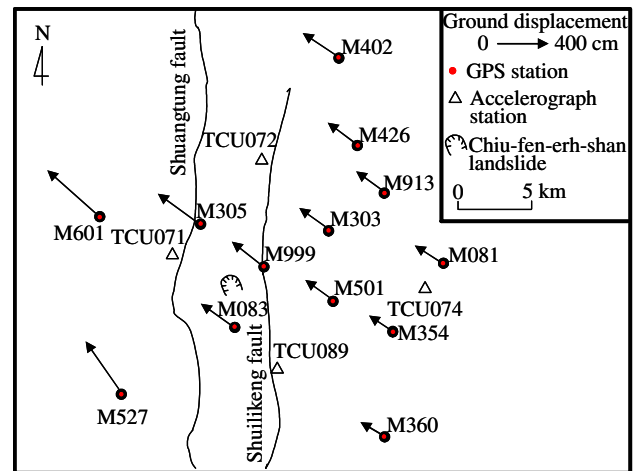


Fig. 8 Spatial distribution of GPS stations in Taiwan

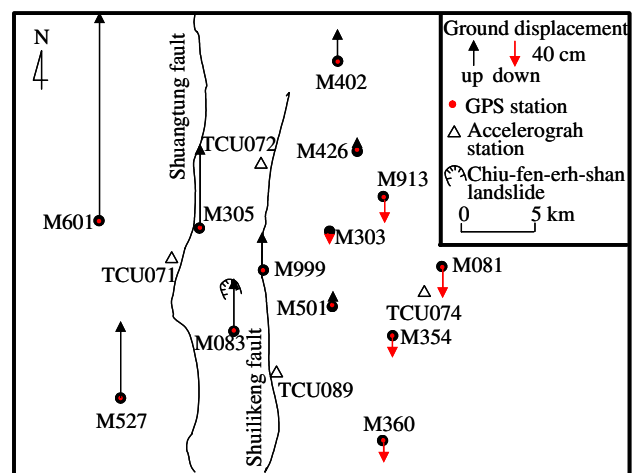
the likely a cause. Regardless, additional modifications to the computation of velocities and displacements from the seismic accelerations are required.

This study follows the baseline-correction method suggested by Ma and Mori (2000) to modify acceleration data. Each accelerograph data set is 90 s long and includes 20 s of pre-event data (<http://scman.cwb.gov.tw/obs/tsmip.htm>). Take the vertical velocities of station TCU072 as an example (Fig. 10a). Line 1 is the line fitted to the pre-event data of velocity data, while Line 2 is computed from the final 20 s. Lines 1 and 2 extended intersect at point A. Prior to point A, the slope of Line 1 is used to correct the pre-event acceleration shifts, whereas Line 2 is used to correct the baseline after point A. The baseline-corrected TCU072 accelerogram is then transformed into velocities and is double integrated into displacements the results of which are shown in Fig. 10b. This correction strategy was applied to all the near by accelerograph data sets.

Station TCU071 is geologically located in the outer foothill zone, while station TCU072 is in the inner foothill zone (Fig. 1). Stations TCU074 and TCU089 are located in the Hsuehshan range. The integrated vertical displacements of each free-field station were compared with the neighboring GPS stations displacement results in the same geological zone. Except for GPS M601, near the station TCU071, the integrated displacements agree well with nearby GPS data (dashed lines in Fig. 11) and successfully capture the downward movement at station TCU074. Moreover, the integrated vertical displacements also decrease from the outer foothill zone, inner foothill zone, to the Hsuehshan range, reproducing the trend seen in the



(a) Horizontal displacement



(b) Vertical displacement

Fig. 9 Ground displacements near the Chiu-fen-erh-shan landslide slope

GPS data. Of particular note, the N–S, E–W, and vertical displacements derived from station TCU072 closely follow those of M305, and M999 GPS stations near the Chiu-fen-erh-shan landslide slope (Fig. 12). Therefore, although the distance from station TCU072 to the landslide slope is greater than those from stations TCU071 or TCU089 (Table 2), TCU072 is in the same geological zone as the Chiu-fen-erh-shan landslide and matches the independent GPS measurements well. Therefore, station TCU072 appears to be the best-fit acceleration data for Chiu-fen-erh-shan landslide simulation.

Shear strength parameters evaluation of the sliding surface

In this study, the displacement-based analysis methods are conducted to evaluate the shear strengths parameters of the

Table 3 GPS measured ground displacements

Station	Upward displacement (cm)	Eastward displacement (cm)	Northward displacement (cm)
M081	−49.0	−197.0	125.0
M083	74.9	−235.2	167.8
M303	−8.1	−207.9	147.7
M305	129.3	−306.0	221.8
M354	−32.7	−181.3	123.5
M360	−31.7	−164.7	95.8
M402	47.9	−253.1	169.4
M426	14.9	−218.1	162.8
M501	4.4	−193.8	140.8
M527	119.9	−262.7	376.9
M601	323.8	−378.1	337.0
M913	−36.2	−200.2	145.8
M999	55.2	−231.8	184.3

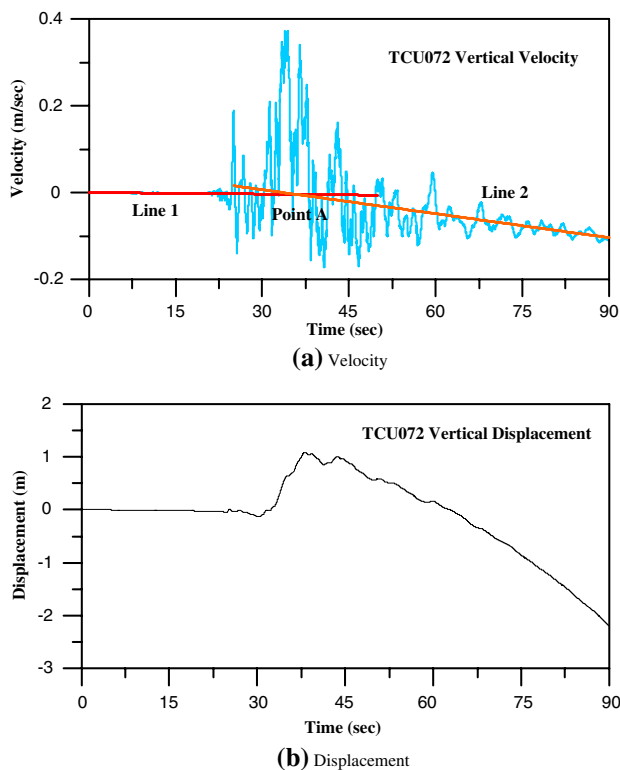


Fig. 10 Data drift with pre-event offset correction

Chiu-fe-erh-shan landslide surface. The displacement-based analysis methods are briefly classified into Newmark sliding model (Newmark 1965) and empirical displacement attenuation formula (Ambraseys and Srbulov 1995). The former gives a simple analytical approach if the seismic data of a nearby accelerogram is available. The latter provides a statistical formula for the seismic slope analysis without neighboring acceleration record.

Newmark sliding model

Newmark (1965) proposed a displacement-based analysis method to calculate the permanent displacement of a translation block under horizontal ground acceleration $a(t)$. The displacement is calculated from two inputs: the critical acceleration A_c and a strong-motion seismogram, a record of the seismic ground acceleration as a function of time $a(t)$. The equation of motion of a rigid block on a cohesionless sliding plane with an inclination angle θ is (Crespellani et al. 2003):

$$\ddot{x}(t) = [a(t) - A_c] \frac{\cos(\phi - \theta)}{\cos \phi} \tag{1}$$

where $\ddot{x}(t)$ is the relative acceleration between the block and the sliding plane and ϕ the friction angle between the sliding mass and the sliding surface. The term $IA = \cos(\phi - \theta) / \cos \phi$ is constant and becomes $IA = 1$ in the specific case of a horizontal sliding surface. A_c , the critical acceleration, can be expressed in (2) for a cohesive surface of an infinite slope failure:

$$A_c = \frac{\frac{c}{d\gamma \cos \theta} + \tan \phi - \tan \theta}{1 + \tan \phi \tan \theta} g \tag{2}$$

in which γ is the unit weight of the rock mass, c indicates the cohesion, and d the thickness of the layer of rock mass in motion, measured perpendicular to the ground surface. g the acceleration of gravity. In addition, when the sliding plane is cohesionless, Eq. 2 can be rewritten:

$$A_c = \frac{\tan \phi - \tan \theta}{1 + \tan \phi \tan \theta} g = \tan(\phi - \theta)g \tag{3}$$

Wilson and Keefer (1983) mentioned that so long as $a(t) < A_c$, the friction-block remains stationary relative to the slope. Once $a(t) > A_c$ (point t_1 , Fig. 13), the block undergoes an acceleration (downslope positive) and

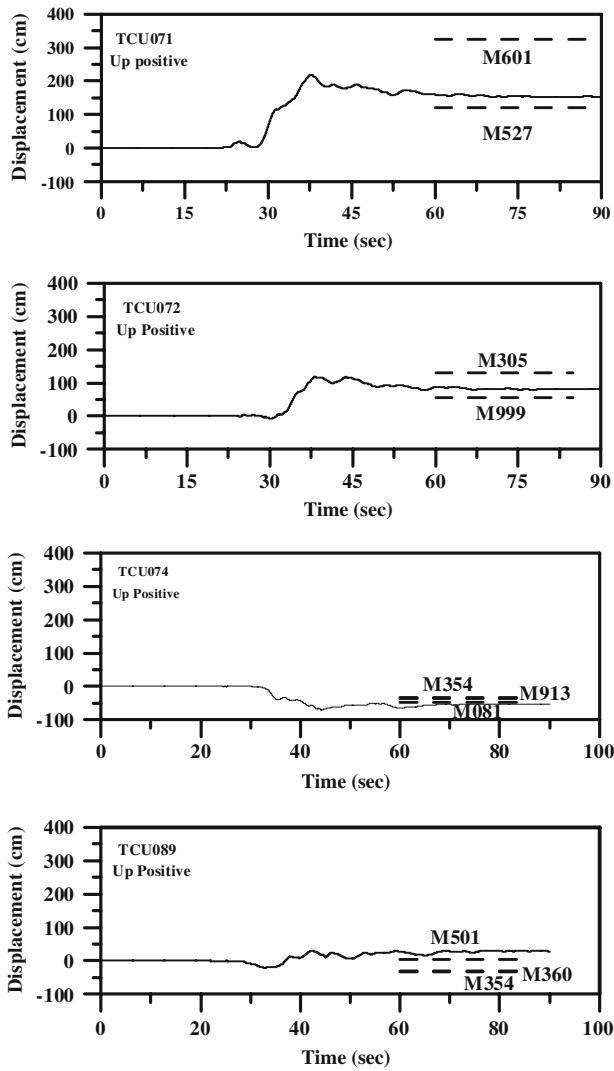


Fig. 11 Comparisons of vertical displacements from acceleration integrations and GPS

continues to accelerate until $a(t)$ again falls below A_c (point t_2 , Fig. 13). During this pulse of $a(t) > A_c$, the velocity of the block may be calculated by integrating the block acceleration over time. Beyond point t_2 , where $a(t)$ again falls below A_c , the block is still moving, but it is now decelerating until the block stops at point t_3 (Fig. 13). Once the block is again stationary, it cannot be displaced again until the next time that $a(t) > A_c$ (Fig. 13). The displacement for a single pulse of ground acceleration exceeding A_c may be found by integrating the block's velocity over time from time $t = t_1$ until $t = t_3$ (Fig. 13).

Empirical displacement attenuation formula

The empirical displacement attenuation formula provides a useful procedure in identifying the landslide hazards of slope displacement under a seismic impact, especially

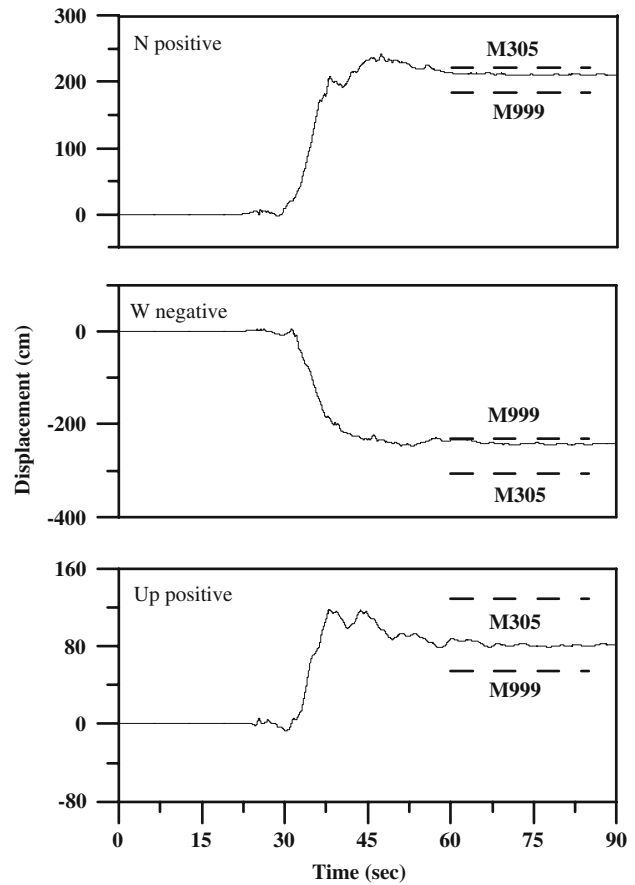


Fig. 12 Displacements of TCU072 and GPS stations near Chiu-fen-erh-shan landslide

when the nearby accelerograph data are not available (Jibson et al. 1998). Ambraseys and Srbulov (1995), after examining 76 world-wide distributed shallow earthquakes (depth <25 km) proposed the following formulas to calculate the two types of displacement: (u_1) due to a one-way, down-slope displacement and (u_2) due to a two way, horizontal displacement on level ground. In the computation of u_1 , asymmetrical sliding is allowed to develop only in one direction, simulating the down-slope movement of a soil mass. The value of u_1 is the maximum cumulative slip caused by a particular time-history. In the computation of u_2 symmetrical displacement representing level ground conditions, slip is allowed to occur in both directions with reversals. The value of u_2 represents the maximum horizontal cumulative displacement attained during a particular earthquake time-history (Ambraseys and Srbulov 1995).

$$\log(u_1) = -2.41 + 0.47M_s - 0.01r + \log\left[(1 - q)^{2.64}(q)^{-1.02}\right] + 0.58p \tag{4}$$

$$\log(u_2) = -2.07 + 0.47M_s - 0.012r + \log(1 - q)^{2.91} + 0.60p \tag{5}$$

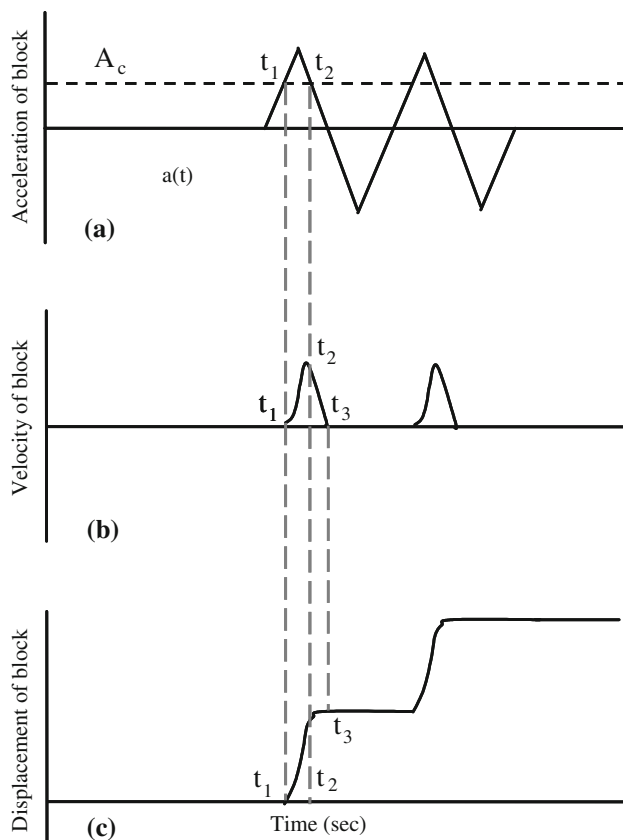


Fig. 13 Demonstration of the Newmark-analysis algorithm

where u_1 and u_2 are displacements in centimeters. M_s is the surface wave magnitude of the earthquake. r is computed using $r = \sqrt{R^2 + h^2}$ where h the focal depth and R the source distance, all in kilometers. q represents the critical acceleration ratio A_c/A_m , i.e. from the ratio of the maximum horizontal acceleration beyond which yielding of the slope material will occur (A_c) to the maximum horizontal ground acceleration of the input ground motion time history (A_m). p is an index of curve fitting and is zero for the best fitted curve.

Chen et al. (2002) modified the empirical displacement attenuation formula for Taiwan by examining the local earthquake-induced slope failures including the Chi-Chi earthquake. The regressed equation is shown as follows:

$$\log(u) = -5.844 + 2.203 \log(1 - q) - 1.056 \log(q) + 1.006M_L - 0.015r + 0.409p \quad (6)$$

where, u is the cumulative horizontal displacement in centimeters. M_L is Richter scale earthquake magnitude.

Shear strength parameters of the Chiu-fen-erh-shan landslide slope

Equations 1–6 imply that the earthquake-induced cumulative displacement of a specific natural slope is a function of

the shear strength parameters of sliding surface because other parameters which are constants of the landslide slope during the earthquake such as earthquake accelerations, Richter scale magnitude, focal distance, and the inclination angle of the sliding surface. In addition, the co-seismic movement of the slope can be calculated by the Newmark sliding model and the empirical displacement attenuation formula. Thus, the shear strength parameters of the Chiu-fen-erh-shan landslide are not expected to change the displacement.

Table 4 lists the key values for co-seismic displacement calculations for the Chiu-fen-erh-shan landslide during the Chi-Chi earthquake. The distance between the seismic source of the Chi-Chi earthquake and the Chiu-fen-erh-shan landslide is 12.3 km calculated from their geographic coordinates. The landslide slope is assumed to be an infinite slope since the length is much larger than the thickness of the sliding block as shown in Fig. 2a. In addition, Wang et al. (2003) identified abnormal cracks and scarps suggesting that Chiu-fen-erh-shan landslide slope failure progressed along the slope based on comparisons with aerial photographs before the Chi-Chi earthquake. Thus, the cohesive strength parameter is assumed 0 kPa in this study based upon this reported residual state. The critical acceleration is calculated using Eq. 3. The horizontal accelerogram paralleling to the dip direction of the Chiu-fen-erh-shan landslide slope is plotted in Fig. 14. This is useful for co-seismic displacement analysis because Eq. 6 evaluates the horizontal, cumulative co-seismic displacement of a landslide. The negative accelerations indicate the direction of S55°E outward from the slope. The maximum horizontal acceleration is 4.14 m/s^2 .

Figure 15 demonstrates the calculated cumulative co-seismic horizontal displacements with friction angles from 24° to 30°. The solid line with hollowed circles is the result of Eq. 6, while the dashed line with solid triangle is obtained from the Newmark sliding model. The two lines intersect at point P for friction angle $\phi = 24.8^\circ$ and the co-seismic displacement of 2.6 m.

Wilson and Keefer (1983) suggested that 10 cm of cumulative displacement calculated using Newmark's method is a conservative estimation of shear strength parameters for macroscopic slope failure. Chen et al. (2004) assumed 5 cm as critical displacement for slope failures in central Taiwan during the Chi-Chi earthquake. The calculated co-seismic displacement of 2.6 m at Chiu-fen-erh-shan landslide slope exceeds the critical displacement when $c = 0 \text{ kPa}$ and $\phi = 24.8^\circ$. This analysis result correlates well with the occurrence of Chiu-fen-erh-shan landslide during the Chi-Chi earthquake. In addition, because the $\phi = 24.8^\circ$ is larger than the inclination angle of the Chiu-fen-erh-shan landslide surface, $\theta = 23^\circ$, the evaluated shear strength parameters can also be applied to

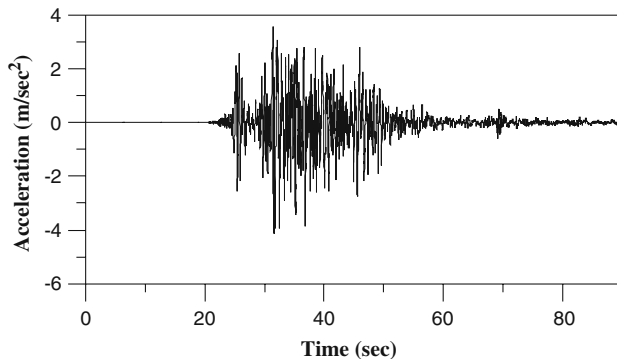
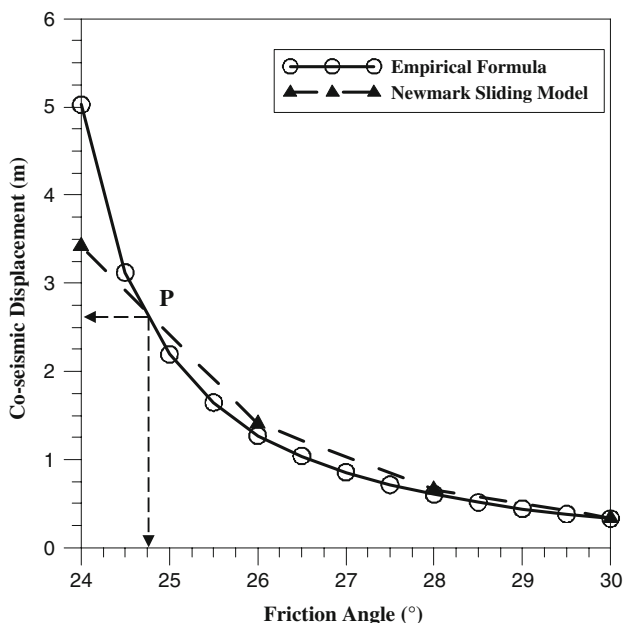
Table 4 Data about the Chiu-fen-erh-shan landslide and Chi-Chi earthquake

Chiu-fen-erh-shan landslide		Chi-Chi earthquake ^a	
Location	N23.96°, E120.83° ^b	Epicenter	N23.85°, E120.82°
Inclination angle (°)	23°	Focal depth (km)	8
–	–	M_L	7.3

^a Central weather bureau of Taiwan (<http://www.cwb.gov.tw/>)

^b Huang et al. (2000b)

^c Figure 2

**Fig. 14** Horizontal accelerogram for Newmark sliding model**Fig. 15** Co-seismic displacements calculated by Newmark sliding model and empirical displacement formula

explain the reason why no remarkable landslide happened before the Chi-Chi earthquake. Furthermore, the shear strength parameters derived here compare well with the available those given in Table 1.

Conclusions

High-density, free-field, strong-motion and GPS stations in Taiwan captured data during the Chi-Chi earthquake which was coincident with the Chiu-fen-erh-shan landslide. These high-quality data enable us to use of the Chiu-fen-erh-shan landslide as a case study to investigate determining the best-fit acceleration data for and the analysis of seismically induced landslides. Using the accelerogram at the shortest distance from a landslide site is a practical approach for analyzing earthquake-induced landslides; however, this study shows that distance between a landslide site and accelerograph station is not a unique factor. Local geology and rock mass must also be considered, especially in areas with complex geology.

This study also used the results from the Newmark's block slide model as well as an empirical displacement attenuation formula to back-calculate the shear strength parameters of an earthquake-induced landslide surface. The analysis results show that the cohesion is 0 kPa and the friction angle is 24.8° for the Chiu-fen-erh-shan landslide. Moreover, the shear strength parameters correlate well with the slope behavior before and under the impacts of Chi-Chi earthquake. The shear strength parameters computed in this analysis compare well with the available those given in the literature. This study also demonstrates the value of collocated GPS and free-field accelerograph stations.

Acknowledgments This work was supported by National Science Council of Taiwan under Contract No. 95-2221-E-006-178 and the Landmark Project of National Cheng Kung University, Taiwan under No. C0043. Professor Kuo-Fong Ma of the Department of Earth Science & Institute of Geophysics, National Central University, Taiwan, is appreciated for her theoretical discussions. Special appreciations will give to the reviewers for their valuable comments.

References

- Ambraseys N, Srbulov M (1995) Earthquake induced displacements of slopes. *Soil Dyn Earthquake Eng* 14(1):59–71. doi:10.1016/0267-7261(94)00020-H
- Boore DM (2001) Effect of baseline corrections on displacements and response spectra for several recordings of the 1999 Chi-Chi,

- Taiwan, earthquake. *Bull Seismol Soc Am* 91(5):1199–1211. doi:[10.1785/0120000703](https://doi.org/10.1785/0120000703)
- Cai Z, Bathurst RJ (1996) Deterministic sliding block methods for estimating seismic displacements of earth structure. *Soil Dyn Earthquake Eng* 15(4):255–268. doi:[10.1016/0267-7261\(95\)00048-8](https://doi.org/10.1016/0267-7261(95)00048-8)
- Chang KJ, Taboada A, Lin ML, Chen RF (2005) Analysis of landsliding by earthquake shaking using a block-on-slope thermo-mechanical model: example of Jiufengershan landslide, central Taiwan. *Eng Geol* 80(1–2):151–163. doi:[10.1016/j.enggeo.2005.04.004](https://doi.org/10.1016/j.enggeo.2005.04.004)
- Chen H (2000) Engineering geological characteristics of Taiwan landslides. *Sino-Geotech* 79:59–70 (in Chinese)
- Chen SM, Loh CH (2007) Estimating permanent ground displacement from near-fault strong-motion accelerograms. *Bull Seismol Soc Am* 97(1B):63–75. doi:[10.1785/0120060060](https://doi.org/10.1785/0120060060)
- Chen ST, Lee ST, Peng WF (2004) A study on the modeling of the earthquake-induced landslide hazard assessment by cumulative displacement method—a case study. In: Proceedings of international symposium on landslides and debris flow hazard assessment. Taipei, Taiwan, pp 3–1–3–15
- Chen ST, Wang SJ, Peng WF, Su JY (2002) Study the failure behavior of the natural slopes under earthquake condition by displacement method. In: Proceedings of seismic slope failure behavior and mitigating countermeasures. Taipei, Taiwan, pp 25–59
- Chigira M, Wang WN, Furuya T, Kamai T (2003) Geological causes and geomorphological precursors of the Tsaoling landslide triggered by the 1999 Chi-Chi earthquake, Taiwan. *Eng Geol* 68(3–4):259–273. doi:[10.1016/S0013-7952\(02\)00232-6](https://doi.org/10.1016/S0013-7952(02)00232-6)
- Chigira M, Yagi H (2006) Geological and geomorphological characteristics of landslides triggered by the 2004 Mid Niigata prefecture earthquake in Japan. *Eng Geol* 82(4):202–221. doi:[10.1016/j.enggeo.2005.10.006](https://doi.org/10.1016/j.enggeo.2005.10.006)
- Crespellani T, Facciorusso J, Madiari C, Vannucchi G (2003) Influence of uncorrected accelerogram processing techniques on Newmark's rigid block displacement evaluation. *Soil Dyn Earthquake Eng* 23(6):415–424. doi:[10.1016/S0267-7261\(03\)00065-4](https://doi.org/10.1016/S0267-7261(03)00065-4)
- Graizer VM (2005) Effect of tilt on strong motion data processing. *Soil Dyn Earthquake Eng* 25(3):197–204. doi:[10.1016/j.soildyn.2004.10.008](https://doi.org/10.1016/j.soildyn.2004.10.008)
- Huang CS, Chen MM, Tsao SJ, Hsu MI (2000a) The large Chiufenershan landslide, Kuoshin Township, Nantou, landslide disasters of Taiwan, 1. Central Geological Survey. MOEA, Taipei (in Chinese)
- Huang CS, Shea KS, Chen MM (2000b) Explanatory text of the geologic map of Taiwan scale 1:50,000 sheet 32 PULI. Central Geological Survey. MOEA, Taipei (in Chinese)
- Huang CC, Lee YH, Liu HP, Keefer DK, Jibson RW (2001) Influence of surface-normal ground acceleration on the initiation of the Jih-feng-erh-shan landslide during the 1999 Chi-Chi, Taiwan, earthquake. *Bull Seismol Soc Am* 91(5):953–958. doi:[10.1785/0120000719](https://doi.org/10.1785/0120000719)
- Hung JJ, Lin ML, Chen TC, Wang KL (2000) Disasters, characteristics and case analysis of slope failures caused by Chi-Chi earthquake. *Sino-Geotechnics* 81:17–32 (in Chinese)
- Jibson RW, Harp EL, Michael JA (1998) A method for producing digital probabilistic seismic landslide hazard maps: an example from the Los Angeles, California, Area. US Geological Survey, Open-File Report 98-113, USA
- Kondo K, Hayashi S (2002) Slope stability analysis. In: Hayashi S (ed) Mountainous disasters triggered by Taiwan earthquake in 1999. Mie, Japan, pp 260–273 (in Japanese)
- Ma KF, Mori J (2000) Rupture process of the 1999 Chi-Chi, Taiwan earthquake from direct observations and joint inversion of strong motion, GPS and teleseismic data. 2000 Western Pacific Geophysics Meeting, WP104–105
- Ma KF, Brodsky EE, Mori J, Chen J, Song TRA, Kanamori H (2003) Evidence for fault lubrication during the 1999 Chi-Chi, Taiwan, Earthquake Mw (7.6). *Geophys Res Lett* 30(5):1244. doi:[10.1029/2002GL015380](https://doi.org/10.1029/2002GL015380)
- Newmark NM (1965) Effect of earthquakes on dams and embankments. *Geotechnique* 15(2):139–159
- Shin TC, Kuo KW, Lee WH, Teng TL, Tsai YB (2000) A preliminary report on the 1999 Chi-Chi (Taiwan) earthquake. *Seismol Res Lett Seismol Soc Am* 71:24–30
- Shou KJ, Su MB, Wang CF (2001) On the stability of the residual slopes of the Chiufengershan landslide. *Sino-Geotechnics* 87:25–30 (in Chinese)
- Shou KJ, Wang CF (2003) Analysis of the Chiufengershan landslide triggered by the 1999 Chi-Chi Earthquake in Taiwan. *Eng Geol* 68(3–4):237–250. doi:[10.1016/S0013-7952\(02\)00230-2](https://doi.org/10.1016/S0013-7952(02)00230-2)
- Wang WN, Chigira M, Furuya T (2003) Geological and geomorphological precursors of the Chiu-fen-erh-shan landslide triggered by the Chi-Chi earthquake in central Taiwan. *Eng Geol* 69(1–2):1–13. doi:[10.1016/S0013-7952\(02\)00244-2](https://doi.org/10.1016/S0013-7952(02)00244-2)
- Wilson R, Keefer DK (1983) Dynamic analysis of a slope failure from the 6 August 1979 Coyote lake, California, Earthquake. *Bull Seismol Soc Am* 73(3):863–887
- Wu JH, Wang WN, Chang CS, Wang CL (2005) Effects of strength properties of discontinuities on the unstable lower slope in the Chiu-fen-erh-shan landslide, Taiwan. *Eng Geol* 78(3–4):173–186. doi:[10.1016/j.enggeo.2004.12.005](https://doi.org/10.1016/j.enggeo.2004.12.005)
- Wu JH (2007) Applying discontinuous deformation analysis to assess the constrained area of the unstable Chiu-fen-erh-shan landslide slope. *Int J Numer Anal Methods Geomech* 31(5):649–666. doi:[10.1002/nag.548](https://doi.org/10.1002/nag.548)
- Yang M, Rau RJ, Yu JY, Yu TT (2000) Geodetically observed surface displacements of the 1999 Chi-Chi, Taiwan, earthquake. *Earth Planets Space* 52:403–413

Author Biography



Jian-Hong Wu received the Bachelor degree from the Department of Mineral and Petroleum Engineering (1996) and Master degree (1998) from the Department of Civil Engineering at the National Cheng Kung University in Taiwan. He received the Ph.D. degree (2003) from the School of Civil Engineering at the Kyoto University in Japan. He has been an assistant professor in the Department of Civil Engineering at the National Cheng Kung University. His research interests are the engineering geology, seismic geotechnics, and discrete numerical analysis methods.